Highlights (3 to 5 bullet points (maximum 85 characters including spaces per bullet point)

- Landscape position units are universal PMA identification units finer than subbasins.
- A Markov chain-based surrogate model of SWAT+ is developed to identify PMAs.
- SWAT+ is qualified to provide the flow distribution matrix among LSUs and channels.
- LSU-based PMAs are more effective in distribution and cumulative load contribution.
- LSU-based PMAs have general applicability for diverse geographic environments.

1. Introduction

Priority management areas (PMAs) are prioritized areas for pollution management in a watershed with a high contribution to the pollutant load of its direct or indirect downstream water bodies (Chen et al., 2014). This concept is similar to a critical source area (CSA), which is more commonly used to identify highly polluted areas (Pionke et al., 2000; White et al., 2009) but usually does not emphasize propagation effects from upstream to downstream in the watershed, which is essential for decision making for comprehensive watershed management. Priority management areas are ideal spatial locations for implementing suitable best management practices (BMPs) to effectively control ecological and environmental problems, such as soil erosion and non-point source pollution (Shen et al., 2015; Tian et al., 2020; Guo et al., 2022). The identification of PMAs can be regarded as the first step in the spatial configuration of BMPs for comprehensive watershed management, where factors affecting actual management decisions, such as investment plans, stakeholder willingness, environmental goals, and BMP effectiveness, can be considered. The spatial distribution of PMAs considerably affects the locations, areas, and effectiveness of the configured BMPs, affecting the cost effectiveness of the BMP scenario (i.e., the spatial configuration of multiple BMPs in the watershed) (Chiang et al., 2014; Qin et al., 2018; Wang et al., 2016; Zhu et al., 2021). Therefore, the accurate identification of PMAs is a key issue for comprehensive watershed management (Chen et al., 2022).

Although field observation is the most accurate approach to investigating the pollutant released at the plot or farm level, the pollutant contributions from upstream plots or farms to downstream channels are difficult or even impossible to observe directly. Therefore, the PMA identification methods are primarily based on watershed modeling. The ~~most important step~~key point in the identification methods~~ying PMAs~~ is to determine an appropriate type of spatial unit~~s~~ as a ~~computing~~ modeling unit for pollutant production and contribution to the assessment outlet, such as the watershed outlet (hereafter referred to as the identification units) (Dong et al., 2018; White et al., 2009). The identification units utilized in existing research are mainly based on three concepts: subbasins (Shang et al., 2012; Chen et al., 2014; Shen et al., 2015; Dong et al., 2018), artificial geographic entities (Tian et al., 2020), and grid cells (Kovacs et al., 2012). It is worth noting that the identification units are not necessarily consistent with the realistic implementation units of BMPs or the simulation units of watershed models (Zhu et al., 2019). For example, the nonstructural BMP of returning farmland to forest configured on the PMA (identified by subbasin units) is implemented on the farmland with a slope above 15° within this subbasin and represented at HRU units using the Soil and Water Assessment Tool (SWAT) (Chen et al., 2022).

A subbasin represents a relatively closed and independent geographic unit that is linked to other subbasins through channels. Subbasin units are the most straightforward and frequently used identification units because they are delineated and modeled in most watershed modeling. In addition to directly utilizing subbasin units, researchers also use the combination of subbasins as identification units according to administrative regions (such as villages; Shang et al., 2012), for the benefit of making and implementing watershed management policies, especially in large study areas (Liu et al., 2019; Shang et al., 2012). However, a subbasin can be recognized and modeled as an integral of one or more levels of finer spatial units to better represent spatial heterogeneity within the subbasin, such as hillslopes, slope position units, landuse fields, and even grid cells. Therefore, it may be too coarse to use these subbasin-based identification units because the heterogeneity of pollutant sources and transportation processes within the subbasins should be considered (Qin et al., 2018; Wang et al., 2016).

Artificial geographic entities refer to artificially constructed and hydrologically connected geographic entities based on the characteristics of a specific geographic environment (Ghebremichael et al., 2013), such as polders that developed in lowland plains with densely distributed rivers and lakes (Tian et al., 2020). Such spatial units have relatively homogeneous features from the perspectives of physical geographic processes and/or anthropogenic activities. For example, a polder may contain agricultural land, irrigation channels, ponds, and even villages, that are enclosed by artificial dams to serve as conservation areas for flood management and waterlogging. Although artificial geographic entities are more appropriate for use as identification units than subbasins in the corresponding geographic environments, they are not easily generalized as universal identification units and, thus, cannot be widely applied to diverse geographic environments.

Grid cells are commonly used spatial units with regular shapes in geographic modeling, and their underlying surface characteristics are homogeneous. Grid cells are universal units to identify PMAs accurately using those watershed models that explicitly represent flow routing among grid cells (Kovacs et al., 2012). However, using grid cells may cause more fragmentized distributions of PMAs, which reduces the implementation efficiency and limits further application (e.g., for PMA-based spatial optimization of BMPs).

Therefore, the existing spatial units used for identifying PMAs cannot balance general applicability to diverse geographic environments and the representation degree of spatial heterogeneity. According to the foregoing analysis, proper identification units should (1) be broadly available and not be limited to a specific geographic environment; (2) be capable of representing the spatial heterogeneity of underlying surface characteristics, physical geographic processes, and/or anthropogenic activities inside the study area by a small number of units; and (3) have hydrologic connections among each other that existing watershed models can explicitly represent.

This study proposes the use of landscape positions along hillslopes within each subbasin to identify PMAs. In this study, landscape positions refer to the geographic objects that reflect the integrated effects of hillslope processes on topography and affect geographic processes on the surface (Volk et al., 2007; Arnold et al., 2010; Miller and Schaetzl, 2015; Qin et al., 2018). Landscape position units are universal in most geographic environments that can be delineated by slope position units (Wolock et al., 2004; Volk et al., 2007; Qin et al., 2009). Based on commonly used classification systems of slope positions (e.g., the divide, backslope, and valley units utilized by Arnold et al. (2010)), each subbasin needs only a few spatial units (e.g., three) to represent the spatial homogeneity from the perspective of hillslope processes (Qin et al., 2018; Rathjens et al., 2016). In addition, landscape position units have inherent upstream-downstream relations among each other, which have been considered in watershed modeling (Arnold et al., 2010; Bieger et al., 2019; Rathjens et al., 2015; Yang et al., 2002) and spatial optimization of BMPs (Qin et al., 2018; Zhu et al., 2019, 2021). Thus, landscape position units meet the requirements for use as the aforementioned identification units.

This study proposes a PMA identification method based on landscape position units ~~exemplified by SWAT+ (i.e., the restructured and enhanced version of the Soil and Water Assessment Tool)~~ and evaluates the effectiveness of the proposed method by comparing it with the adoption of ~~to~~ widely used subbasin units. The remainder of this paper is organized as follows: Section 2 introduces the proposed method together with the exemplified implementation based on the SWAT+ model (i.e., the restructured and enhanced version of the SWAT model; Bieger et al., 2017, 2019); and Section 3 presents a comparative experimental design of using landscape position and subbasin units to identify PMAs of total nitrogen in two watersheds with different geographic characteristics. The experimental results and discussion are presented in Section 4, and the conclusions are presented in Section 5.

2. Method design

To identify PMAs at the landscape position unit level, two key issues must be addressed. The first is the quantification of pollutants released from the landscape position units. The second is how to distinguish the pollutant load contribution of each landscape position unit to the assessment outlet, that is, the residual amount of pollutant after being transported to its direct downstream channel and then transitioning in hierarchical channels before reaching the assessment outlet (Chen et al., 2014).

Generally, the contribution of the pollutant load cannot be directly determined from the results of most watershed models. Instead, watershed models output the pollutant released from each simulation unit (e.g., the hydrologic response unit [HRU] in SWAT) or lumped unit (e.g., subbasin), as well as the flow of substances in and out of each channel. To fill this gap, Grimvall and Stålnacke (1996) proposed a Markov chain-based surrogate model to simulate pollutant transitions from upstream channels (one channel for each subbasin) to the assessment outlet in a statistical manner. Their basic idea is to use analog pollutant transformation and transfer processes in hierarchical channels as a Markov process, in which, the transition matrix is determined by the upstream-downstream relations among channels and the retention effects of the channel routing process. After a finite number of transitions (equal to the length of the longest branch in hierarchical channels), all pollutants from upstream subbasins reach the assessment outlet, thus, the corresponding pollutant load contributions can be derived (Grimvall and Stålnacke, 1996).

Follow-up studies continued to apply the subbasin unit in the Markov chain-based model (Chen et al., 2014; Rankinen et al., 2016), which includes pollutant production on hillslopes and pollutant routing in the channel. The transition matrix of the Markov chain-based model can be improved to represent both landscape position and channel units. Therefore, if these two processes can be separated in the landscape position units and channels, the improved Markov chain-based model will be able to distinguish the pollutant contribution of each landscape position unit to the assessment outlet. Based on this basic idea, the proposed method aims to incorporate a watershed model that supports landscape position units as simulation or lumped units, to improve the Markov chain-based PMA identification method from the subbasin level to the landscape position unit level. Therefore, the Markov chain-based PMA identification method can be generalized as a method framework that supports one or more types of hierarchical spatial units with explicit hydrological connections (i.e., upstream-downstream relations), such as subbasins and landscape position units (Fig. 1).

In this study, the exemplified implementation of the improved Markov chain-based PMA identification method adopted the SWAT$^+$ model to construct the transition matrix and quantify the pollutants released. Section 2.1 first introduces the ability of the SWAT$^+$ model to delineate and represent landscape position units. Section 2.2 then elaborates on the proposed method to derive pollutant load contribution of landscape position units to the watershed outlet, taking the SWAT$^+$ model as an implementation example.

2.1 Delineation and modeling of landscape position units in SWAT$^+$

As a restructured and enhanced version of the SWAT model, SWAT$^+$ (Bieger et al., 2017, 2019) introduced a new type of spatial unit between the subbasin unit and HRU named the landscape position unit (LSU), which includes the uplands and floodplains (Fig. 2). SWAT$^+$ uses the relative position index (RPI) of each cell in a gridded digital elevation model (DEM) to delineate LSUs (Rathjens et al., 2016). The RPI of each cell is the ratio of the drop length to its downstream valley (i.e., the stream cell) and the length from its upstream ridge cell to the same valley cell. The RPI ranges from 0 to 1. The cell with a RPI less than the user-specific threshold is classified as the floodplain. This means that the basic spatial discretization of a watershed in SWAT$^+$ contains three types of nested spatial units as a hierarchy: subbasin, LSU, and HRU. The HRU, as the basic simulation unit of SWAT$^+$, is delineated as the unique combination of soil, land use, and slope class within the LSU, which is spatially discrete (Fig. 2a) and even lacks explicit spatial locations according to different delineation parameters (Arnold et al., 2010). Therefore, HRUs are unsuitable for PMA identification units since there are no hydrologic connections between HRUs, although the HRU is finer than the LSU. In addition, SWAT$^+$ also abstracts specific types of geographic entities as spatial units with locations and properties to participate in watershed modeling. For example, reservoirs or ponds within a subbasin are first generalized as one point in the channel that divides the channel into two parts, and then defined by the upstream part with additional properties such as storage capacity (Fig. 2a). The hillslopes, LSUs, and HRUs also are delineated accordingly, while the two aquifer units remain unchanged (Fig. 2b). These spatial units can enrich the flow routing network of SWAT$^+$ and play important roles in the simulation of study areas with specific geographic environments, such as, agricultural ecosystems with densely distributed ponds.

With the new spatial discretization scheme, SWAT$^+$ improves the representation of realistic hydrologic processes from hillslopes to channels (Bieger et al., 2019).

Instead of directly adding all released substances from HRUs (including water, sediment, and pollutants) to the channel, SWAT$^+$ first lumps HRUs' outputs at the LSU level and then routes these outputs to other spatial units using two different methods. The first method involves completely draining from the upland to the floodplain and from the floodplain to the channel, which is applicable for lateral flow in soils and groundwater recharge in aquifers (Fig. 2b). The second method distributes water from the upland to the channel/pond/reservoir by a constant ratio (e.g., 0.30 from LSU2 to the pond/reservoir and 0.66 from LSU4 to the channel, as shown in Fig. 2b; hereafter 'channel/pond/reservoir' is referred to as channel collectively) and the rest to the floodplain as additional net precipitation to participate in the hydrologic simulation. The output from the floodplain drains entirely into the channel (Fig. 2b). SWAT$^+$ provides two ways to determine this ratio: the user-specified global value for all upland units in the watershed and the area ratio of each upland to its floodplain. The area ratio method has been proven to be more realistic in representing the connectivity than the fixed ratio for the entire watershed (Bieger et al., 2019) and is, therefore, applied in this study.

With the flow routing network primarily constructed by chain of HRU, LSU, and channel (Fig. 2b), SWAT$^+$ is suitable to quantify pollutants released at the landscape position units and the corresponding transportation amounts to their direct channels.

2.2 Pollutant load contribution of landscape position units derived from a Markov chain-based surrogate model of SWAT$^+$

Based on the flow routing network and simulation results of SWAT$^+$, the key part of the Markov chain-based surrogate model can be determined, that is, the transition matrix of pollutants through LSUs and channels. Subsequently, using the lumped simulation results at LSUs as inputs, the Markov chain-based model can determine the pollutant load contribution of each landscape position unit.

2.2.1 Transition matrix of pollutants based on flow routing network and retention effects of the channel routing process

The transition matrix is constructed using flow distribution relations from upstream to downstream units and the retention coefficients of channel routing processes (Chen et al., 2014). According to the spatial discretization scheme of SWAT^{+} (see Section 2.1), the flow distribution relations among the LSUs and channels can be represented by an $n \times n$ matrix H (Eq. 1). Fig. 3 shows an example of the matrix H.

$$H(i,j) = \begin{cases} s, & \text{if LSU(floodplain) } j \text{ is adjacent downstream of LSU(upland) } i \\ 1-s, & \text{if CHA(channel) } j \text{ is directly downstream of LSU(upland) } i \\ 1, & \text{if CHA } j \text{ is adjacent downstream of CHA } i \text{ or LSU(upland) } i \\ 0, & \text{otherwise} \end{cases} \tag{1}$$

where n is the total number of LSUs and channels in the watershed, and s is the flow distribution ratio from upland to floodplain. For surface runoff, s is initially set by the area ratio of upland and hillslope, while for lateral flow and groundwater recharge, s = 1 (Fig. 2b). Each row represents the flow distribution relations of a spatial unit with its downstream units. The sum of all elements in one row equals 1, except for the channel row where the assessment outlet is located (e.g., the 7$^{\text{th}}$ row in Fig. 3, when the outlet of channel 7 is the assessment outlet). For a given assessment outlet of channel k, there exists a smallest integer N_k to make $H^{N_k} = 0$, which means that after N_k transitions, pollutants from all upstream spatial units of channel k will reach the outlet. The physical meaning of N_k is the longest routing length from the uppermost spatial units to the outlet of channel k, for example, $N_7 = 4$ in Fig. 3.

The complicated channel routing process of pollutants accounts for the chemical transformation or retardation of the interested substances. For example, a stepwise transformation from organic nitrogen to ammonia, then to nitrite, and finally to nitrate is simulated in SWAT (Neitsch et al., 2011). For each channel of the study area, the difference between the output substance and the input can be explained by the retention effect of the channel, which is time-varying and affected by pollutant concentration, water temperature, and other factors. The yearly average retention of each channel can be regarded as its stable removal capacity of pollutants calculated as the retention coefficient (Eq. 2) (Chen et al., 2014; Grimvall and Stålnacke, 1996; Hejzlar et al., 2009). The landscape position unit is a lumped unit of pollutant sources calculated at HRUs, thus, it has no retention effect.

$$r = (\mathrm{Load}_{\mathrm{in}} - \mathrm{Load}_{\mathrm{out}})/\mathrm{Load}_{\mathrm{in}} \tag{2}$$

where r denotes the retention coefficient of the channel to a specific pollutant; $\mathrm{Load}_{\mathrm{in}}$ is the pollutant input to the channel that includes pollutant outputs of adjacent upstream channels and pollutant released from upstream LSUs; and $\mathrm{Load}_{\mathrm{out}}$ is the pollutant output at the outlet of the channel.

The retention coefficient of spatial units, R, also is represented by an $n \times n$ matrix, as follows:

$$R = \begin{pmatrix} r_1 & 0 & \cdots & 0 \\ 0 & r_2 & \cdots & 0 \\ \vdots & \vdots & \ddots & \vdots \\ 0 & 0 & \cdots & r_n \end{pmatrix} \tag{3}$$

where the ith diagonal element r_i denotes the retention coefficient of spatial unit i; for LSUs, $r_i = 0$; and for channels, r_i can be calculated using Eq. 2.

The transition matrix, $\tilde{H}$, of the Markov chain-based model can be represented as follows and used to simulate the flow transitions of substances (e.g., water and pollutants) through the hierarchy of landscape position units and channels:

$$\tilde{H} = H\,(I - R) \tag{4}$$

where I is an identity matrix.

2.2.2 Calculation of pollutant load contribution

Except for the transition matrix, the pollutant released from each LSU is the primary input data for the Markov chain-based model as the initial states. Because the channel acts as a receptor for pollutants, it contains no self-generated pollutants. An $n \times 1$ matrix, L, is used to organize the input of the pollutant sources:

$$L = (e_1,\ e_2,\ \cdots,\ e_i,\ \cdots,\ e_n)^{\mathrm{T}} \tag{5}$$

where e_i is the pollutant released from spatial unit i based on the simulation results of SWAT$^+$. Specifically, $e_i = 0$, if i is a channel.

The pollutant load contribution of each spatial unit to a specific assessment outlet can be calculated using simple matrix calculations (Grimvall and Stålnacke, 1996):

$$E = \left(\tilde{H}_k\right)^{N_k} V_k * L \tag{6}$$

$$\tilde{H}_k(i,\ j) = \begin{cases} \tilde{H}(i,\ j), & \text{if } i \neq k \\ 1, & \text{if } i = j = k \\ 0, & \text{if } i = k \text{ and } j \neq k \end{cases} \tag{7}$$

$$V_k(i) = \begin{cases} 1, & \text{if } i = k \\ 0, & \text{otherwise} \end{cases} \tag{8}$$

where k represents the assessment outlet located channel, and the corresponding modification from $\tilde{H}$ to $\tilde{H}_k$ implies that the kth state is transformed to an absorbing state; V_k is an $n \times 1$ matrix for extracting the kth column of the $\left(\tilde{H}_k\right)^{N_k}$, resulting in the contribution rate of each unit; and the asterisk* denotes element-wise multiplication.

Considering that the pollutants of interest may have various states that are modeled in different watershed processes, the calculation of the pollutant load contribution should be combined with all components calculated by different transition matrixes, ***H***, and pollutant source matrixes, ***L***. For example, the total nitrogen consists of organic and inorganic nitrogen. In SWAT/SWAT$^+$, the inorganic nitrogen output in the channel includes ammonia, nitrite, and nitrate nitrogen. The nitrate nitrogen (NO_3) and the organic nitrogen (*ORGN*) are relatively stable forms of nitrogen in the soil that are routed from HRUs into the channel with water and sediment (Neitsch et al., 2011). Since the nitrogen output at the LSU level is the sum of its internal HRUs' output, the nitrogen released from LSUs considered in this study also comprises NO_3 and *ORGN*. For the sake of simplicity, we use the term of total nitrogen (TN) in this study. The TN load contribution can be calculated as follows:

$$E_{TN} = E_{NO3-SURF} + E_{NO3-LAT} + E_{NO3-GW} + E_{ORGN} \tag{9}$$

$$E_{NO3-SURF} = \left(H_{SURF}(I - R_{NO3})_k\right)^{N_k} V_k * L_{NO3-SURF} \tag{10}$$

$$E_{NO3-LAT} = \left(H_{LAT}(I - R_{NO3})_k\right)^{N_k} V_k * L_{NO3-LAT} \tag{11}$$

$$E_{NO3-GW} = (H_{GW}(I - R_{NO3})_k)^{N_k} V_k * L_{NO3-GW} \tag{12}$$

$$E_{ORGN} = (H_{SURF}(I - R_{ORGN})_k)^{N_k} V_k * L_{ORGN-SURF} \tag{13}$$

where *SURF* denotes the surface runoff, *LAT* denotes the lateral flow, *GW* denotes the groundwater recharge; H_{SURF}, H_{LAT}, and H_{GW} describe the flow distribution relations among the spatial units of surface runoff, lateral flow, and groundwater recharge, respectively; $L_{NO3\text{-}SURF}$, $L_{NO3\text{-}LAT}$, and $L_{NO3\text{-}GW}$ are the amounts of NO_3 released in surface runoff, lateral flow, and groundwater recharge, respectively; and $L_{ORGN\text{-}SURF}$ is the amount of *ORGN* released in surface runoff.

2.2.3 PMA identification based on classification of pollution degrees

Once the pollutant load contribution of each landscape position unit is distinguished, a classification of pollution degrees can be determined to identify different levels of PMAs, such as high-, medium-, and low-contribution PMAs. In this study, ~~we adopted~~ the natural breaks method, a commonly used classification method (De Smith et al., 2018; Giri et al., 2016), was used to classify the pollutant load contribution. The natural breaks method ~~classifies~~ groups the data into different classes ~~with~~ utilizing the statistical groupings and pattern characteristics inherent in the data to minimize the data difference within a class and maximize the difference between classes.

3. Experimental design

To illustrate the effectiveness of the proposed method, a comparative experimental study was designed to identify the PMAs for total nitrogen at the landscape position and subbasin levels based on the same calibrated SWAT^{+} model. The source of total nitrogen considered in this study is summed by nitrate nitrogen and organic nitrogen on the LSU. Since the improvement of the Markov-based surrogate model in this study does not change the calculation principle of the original model, the differences in identifying PMAs can be attributed to the identification units adopted (i.e., the LSU and the subbasin unit). The same experimental design was used in two watersheds to evaluate the applicability of the method under different geographic characteristics (e.g., topographical, climatic, hydrological, and ecological conditions), that is, the Zhongtianshe Watershed (~42 km^2) in southern China and the Willow River Watershed (~212 km^2) in western Wisconsin, USA (Fig. 4).

3.1 Study areas and data

The Zhongtianshe Watershed, located south of Liyang, Jiangsu Province, China, is a typical hilly area situated in the upstream region of Taihu Lake ~~Tai~~. The study area is characterized by a subtropical monsoon climate. The average annual temperature is 15.5°C and the average annual precipitation is 1160 mm. The main soil type is yellow-red soil, which is a type of acidic soil that is easily weathered. The main land use types are forest (77%), cropland (10%, primarily rice paddy fields), orchard (3%), residential areas (8%), and water areas (2%). The watershed experiences frequent agricultural activities, and the cultivation of rice and wheat is the primary contributor to local non-point source pollution. Because the study area is in the drinking water source of Liyang, knowing the details of the pollution situation and taking reasonable measures to control pollution is a vital issue for the local government (Shi et al., 2021).

The Willow River, located in western Wisconsin, USA, is a tributary of the St. Croix River. It is classified as part of the Central Wisconsin Undulating Till Plain based on a report by the U.S. Environmental Protection Agency (EPA, 2020), and is characterized as relatively flat compared to the Zhongtianshe watershed. The area has a continental climate with high evapotranspiration, an average annual temperature of 11.8°C, and an average annual precipitation of 788 mm. The soils are predominantly silt loams with moderately well-drained characteristics. The main land use types are grassland (45%), forest (27%), cropland (18%), residential areas (6%), and wetlands (3%). Watershed crops are dominated by corn-silage, soybeans, and alfalfa, resulting in non-point source pollution and relatively poor water quality. As the headwater of the popular Willow River State Park and attractive trout fishing destinations, the watershed has been the focus of non-point source pollution control for decades (Almendinger and Murphy, 2007).

The input data of the study areas for the SWAT$^+$ modeling consisted of a DEM, land use types, soil types and properties, meteorological data, agricultural management practices, and observed data at the watershed outlet. Detailed descriptions of the data for the two watersheds are listed in Table 1.

3.2 Modeling and calibration of the SWAT$^+$ model

Two SWAT$^+$ models were built by QSWAT$^+$ version 1.2.2 and SWAT$^+$ version 59.3 to simulate the total nitrogen pollution in each study area. A total of 15 subbasins, 41 LSUs, and 1260 HRUs were generated in the Zhongtianshe Watershed, while 19 subbasins, 131 LSUs, and 7245 HRUs were generated in the Willow River Watershed

(Fig. 5). The RPI thresholds for delineating uplands and floodplains were manually determined by visual interpretation of contour lines, which are 0.14 and 0.3 for the Zhongtianshe Watershed and the Willow River Watershed, respectively. In most situations, each subbasin has one upland and one floodplain. There may be an additional floodplain due to the very short channel generated after the setting of a pond or reservoir.

Limited by the available observed data for the Zhongtianshe Watershed, the year 2011 was set as a warm-up period, and 2012–2013 and 2014–2015 were set as calibration and validation periods, respectively, for daily flow modeling. The model performance for the total nitrogen was calibrated using the 5-day or 3-day monitoring data from 2014 to 2015 (a total of 181 values, of which 53 values during the rainy season were sampled in about three days interval from June to August in the two years), without validation.

For the Willow River Watershed, the model had a 2-year warm-up period. The calibration period ranged from 1 January 2012 to 31 July 2014, and the validation period was from 1 October 2010 to 31 December 2011, respectively. The available daily ammonia and organic nitrogen were combined to calibrate and validate the nitrogen modeling.

Model performance was evaluated using the Nash–Sutcliffe efficiency (NSE, Nash and Sutcliffe, 1970), percentage bias (PBIAS), root mean square error-standard deviation ratio (RSR), and coefficient of determination (R^2), as listed in Table 2. According to the criteria of monthly model performance proposed by Moriasi et al. (2007), a satisfactory model should generally have the NSE > 0.50;~~,~~ RSR < 0.70;~~,~~ and

PBIAS ±25% for flow, ±55% for sediment, and ±70% for nutrients. Meanwhile, the daily model is more likely to have poorer model performance than the monthly model (Engel et al. 2007). Therefore, considering this study mainly utilizes the relative rather than absolute ~~reliable~~ model result comparisons to verify the effectiveness of the proposed PMA identification method, both calibrated models can be regarded as acceptable for use in the current study. Besides, considering that the SWAT^{+} model is still in active development, ~~we created~~ an open-source repository was created to store the modeling data and update the modeling details and results routinely in future~~our following~~ studies~~y~~ (https://github.com/lreis2415/WatershedModelingData).

3.3 Identification and evaluation of PMAs at LSU level and subbasin level

To evaluate the effectiveness of the PMAs at the LSU level, PMAs also were identified at the subbasin level in the same study area based on the same calibrated SWAT^{+} model and the corresponding Markov chain-based surrogate model.

The average annual total nitrogen modeled during the calibration period was used for the input data of the Markov chain to identify the PMAs, with the watershed outlet set as the assessment outlet. The natural breaks method was utilized to classify the nitrogen load contribution of the spatial units into three classes, and high-contribution areas were identified as PMAs.

The comparison of the PMAs identified at the LSU and subbasin levels was done from two perspectives, the spatial distribution and cumulative load contributions. The spatial distribution of PMAs is an intuitive way to qualitatively analyze the spatial consistency and differences between different units. The cumulative load contributions were used to quantitatively compare the relations between the area of PMAs and their total pollutant load contribution.

4. Experimental results and discussion

4.1 Spatial distribution of PMAs

In the Zhongtianshe Watershed, five LSUs and two subbasins, classified as high-contribution areas, were identified as PMAs (Fig. 6). There was a relatively consistent spatial correlation between the two levels. For example, one subbasin was identified as PMA at both levels, that is, subbasin S2 in Fig. 6b and its two LSUs, L2 and L3 in Fig. 6a. PMAs identified at the LSU level have a more accurate spatial distribution because of the inherent characteristics of the LSUs that can represent the spatial heterogeneity within subbasins. Considering the retention effect of ponds and reservoirs in SWAT$^+$, the upstream part of the subbasin may have a distinctive load contribution compared to the downstream part. For example, in subbasin S1 in Fig. 6b, the upstream part composed of floodplain L10 and upland L12 in Fig. 6a were identified as medium-contribution areas, while the downstream floodplain L1 was the high-contribution area. In addition, most LSU-based PMAs were floodplains in the Zhongtianshe Watershed. This may be because the cropland in the study area is mostly distributed along the valley plain, which is a direct cause of local non-point source pollution. These results also indicate that SWAT$^+$ is well suited for characterizing pollutants released at the LSU level and their transitions in the reconstructed routing network by LSUs and channels (including ponds).

In the Willow River Watershed, two LSUs and two subbasins, classified as high-contribution areas, were identified as PMAs (Fig. 7). It was similar that at both the LSU and subbasin levels the northeast areas of the watershed were identified as low contribution areas, owing to the upstream pollution predominantly reduced by the ponds and wetlands along the main channel. Although the results identified at the two levels had similar spatial distributions, the subbasin-based PMAs covered larger areas than the LSU-based PMAs, which may result in additional screening work or more investment in watershed management decision making. In contrast, the LSU-based PMAs were the upland areas within the subbasins, that is, uplands L1 and L2 (Fig. 7a) within two subbasins (Fig. 7b). The medium-contribution areas identified at the LSU level were also more specific and detailed than the areas identified at the subbasin level. Therefore, it is clear that LSU-based results can provide a finer identification than subbasin-based results in the Willow River Watershed.

In addition, for the Willow River Watershed, LSUs belonging to subbasin L2 in Fig. 7b were not identified as PMAs but as contribution areas classified as medium-contribution areas. This shows that the application of detailed spatial units could decompose the aggregation of the pollutant load within a subbasin in a relatively realistic representation, although subbasin S2 contributed a high pollutant load as the result of being the largest subbasin in the watershed.

Overall, LSU-based PMAs have improved the accuracy of identification from the perspective of spatial distribution compared with subbasin-based PMAs. It is also shown that the proposed PMA identification method at landscape position units using SWAT$^+$ is effective and applicable to different watersheds.

4.2 Cumulative load contribution

To quantitatively evaluate the difference in PMAs identified at the LSU and subbasin levels for each case study, each type of spatial unit was ranked by load contribution in descending order and plotted in Figs. 8 and 9, with the cumulative area and load contribution calculated.

In the Zhongtianshe Watershed, LSU-based PMAs contributed 48.6% of the total nitrogen in 23.3% of the watershed area, whereas subbasin-based PMAs only contributed 44.7% in as much as 30.1% of the area (Fig. 8a). This means that landscape position units are more effective in identifying the PMAs. Moreover, the cumulative area-contribution line of the LSU-based method in Fig. 8a was always higher than that of the subbasin-based method, proving its better effectiveness, although based on different types of identification units.

In the Willow River Watershed, LSU-based PMAs contributed 31.7% of the total nitrogen in 5.9% of the watershed area, whereas subbasin-based PMAs contributed 54.9% of the total nitrogen in 21.5% of the area (Fig. 9a). It is not convincing to simply use these numbers to compare the effectiveness of the two levels in this watershed. However, the line in Fig. 9a shows that the LSU-based PMAs almost always covered less area than the subbasin-based PMAs under the same cumulative contribution. In general, the results reveal that there would be less work on the reduction of pollution at the LSU level if the local government wanted to control the pollution to a certain extent.

Furthermore, there was no deterministic relation between the area of the spatial unit and its pollutant load contribution. For example, LSU L1 in the Zhongtianshe Watershed contributed 12.0% of the total nitrogen but ranked 17 in area, while subbasin S1 contributed 24.3% of the total nitrogen with the 2nd largest area (Fig. 8). In the Willow River Watershed, LSU L1 contributed 16.8% of the total nitrogen with the 2nd largest area, and subbasin S1 contributed 31.7% of total nitrogen with the 2nd largest area of all subbasins (Fig. 9).

Although absolute differences exist in the results of the two watersheds due to different geographic characteristics, the comparison between them is less important for the scope of this study (which is to evaluate the effectiveness of the PMAs at the LSU level). Instead, the similar appearance depicted by the relations between the area of PMAs and their total load contribution at the two levels in different watersheds can also show the universality and effectiveness of LSUs. In summary, identifying PMAs based on landscape positions performs better than subbasins from the perspectives of both the spatial distribution and cumulative load contribution in both test watersheds. Thus, LSU-based PMAs have the merit of accounting for more pollutant load contributions with smaller areas, and can effectively be utilized in the spatial configuration of BMPs for integrated watershed management.

5. Conclusions

This study proposes the use of landscape position units (LSUs), derived from a universal type of spatial unit for most geographic environments, as identification units for priority management areas (PMAs). A Markov chain-based surrogate model of the SWAT^{+} model was implemented with the improvement of the transition matrix in representing both landscape position and channel units to distinguish the pollutant load contribution of each LSU to the assessment outlet and then identify the PMAs according to a classification method. The experimental results show that landscape position units are more effective than widely used subbasins in identifying PMAs because of their superior ability to represent hillslope processes and the spatial heterogeneity of underlying surface environments within subbasins. Therefore, LSU-based PMAs are much more valuable for providing accurate locations for implementing suitable BMPs for integrated watershed management.

The improved Markov chain-based PMA identification method can be regarded as a method framework. More types of spatial units with explicit upstream-downstream relations may be proposed and validated to identify PMAs with the support of proper watershed models. In addition, several issues may be worth attention in future research such as 1) how to consider various climate scenarios to determine the retention effects of channel routing processes; 2) how to better quantify the hydrological connectivity among landscape positions and channels and its effects on PMA identification; 3) how a specific type of identification unit affects PMA identification under different delineation methods; 4) how the modeling accuracy of the same or different watershed models affects PMA identification; and 5) how PMAs derived from different identification units impact the effectiveness and efficiency of the spatial optimization of BMPs.

Acknowledgements

Support for A-Xing Zhu through the Vilas Associate Award, the Hammel Faculty Fellow Award, and the Manasse Chair Professorship from the University of Wisconsin-Madison are greatly appreciated.

Funding

The work reported here was supported by grants from National Natural Science Foundation of China (Project No.: 41871362, 42101480, 41871300), Key Project of Innovation LREIS (Project No.: KPI003), and the 111 Program of China (Approved Number: D19002).

References

Almendinger, J.E., Murphy, M.S., 2007. Constructing a SWAT model of the Willow River watershed, western Wisconsin. St. Croix Watershed Research Station, Science Museum of Minnesota. 84 pp.

Arnold, J., Allen, P., Volk, M., Williams, J.R., Bosch, D., 2010. Assessment of different representations of spatial variability on SWAT model performance. Transactions of the ASABE. 53(5), 1433–1443. https://doi.org/10.13031/2013.34913.

Bieger, K., Arnold, J.G., Rathjens, H., White, M.J., Bosch, D.D., Allen, P.M., 2019. Representing the connectivity of upland areas to floodplains and streams in SWAT+. J. Am. Water Resour. Assoc. 55(3), 578–590. https://doi.org/10.1111/1752-1688.12728.

Bieger, K., Arnold, J.G., Rathjens, H., White, M.J., Bosch, D.D., Allen, P.M., Volk, M., Srinivasan, R., 2017. Introduction to SWAT+, a completely restructured version of the Soil and Water Assessment Tool. J. Am. Water Resour. Assoc. 53(1), 115–130. https://doi.org/10.1111/1752-1688.12482.

Chen, L., Li, J., Xu, J., Liu, G., Wang, W., Jiang, J., Shen, Z., 2022. New framework for nonpoint source pollution management based on downscaling priority management areas. J. Hydrol. 606, 127433. https://doi.org/10.1016/j.jhydrol.2022.127433.

Chen, L., Zhong, Y., Wei, G., Cai, Y., Shen, Z., 2014. Development of an integrated modeling approach for identifying multilevel non-point-source priority management areas at the watershed scale. Water Resour. Res. 50(5), 4095–4109. https://doi.org/10.1002/2013WR015041.

Chiang, L.C., Chaubey, I., Maringanti, C., Huang, T., 2014. Comparing the selection and placement of best management practices in improving water quality using a multiobjective optimization and targeting method. Int. J. Environ. Res. Public Health 11(3), 2992–3014. https://doi.org/10.3390/ijerph110302992.

De Smith, M. J., Goodchild, M. F., Longley, P., 2018. Geospatial analysis: A comprehensive guide to principles, techniques and software tools. 6th edition, England: The Winchelsea Press.

Dong, F., Liu, Y., Wu, Z., Chen, Y., Guo, H., 2018. Identification of watershed priority management areas under water quality constraints: A simulation-optimization approach with ideal load reduction. J. Hydrol. 562, 577–588. https://doi.org/10.1016/j.jhydrol.2018.05.033.

Engel, B., Storm, D., White, M., Arnold, J., Arabi, M., 2007. A hydrologic/water quality model application protocol. J. Am. Water Resour. Assoc. 43(5), 1223–1236. https://doi.org/10.1111/j.1752-1688.2007.00105.x.

Ghebremichael, L.T., Veith, T.L., Hamlett, J.M., 2013. Integrated watershed- and farm-scale modeling framework for targeting critical source areas while maintaining farm economic viability. J. Environ. Manage. 114, 381–394. https://doi.org/10.1016/j.jenvman.2012.10.034.

Giri, S., Qiu, Z., Prato, T., Luo, B., 2016. An integrated approach for targeting critical source areas to control nonpoint source pollution in watersheds. Water Resour. Manage. 30, 5087–5100. https://doi.org/10.1007/s11269-016-1470-z.

Grimvall, A., Stålnacke, P., 1996. Statistical methods for source apportionment of riverine loads of pollutants. Environmetrics 7(2), 201–213. https://doi.org/10.1002/(SICI)1099-095X(199603)7:2<201::AID-ENV205>3.0.CO;2-R.

Guo, Y., Wang, X., Melching, C., Nan, Z., 2022. Identification method and application of critical load contribution areas based on river retention effect. J. Environ. Manage. 305, 114314. https://doi.org/10.1016/j.jenvman.2021.114314.

Hejzlar, J., Anthony, S., Arheimer, B., Behrendt, H., Bouraoui, F., Grizzetti, B., Groenendijk, P., Jeuken, M.H.J.L., Johnsson, H., Lo Porto, A., Kronvang, B., Panagopoulos, Y., Siderius, C., Silgram, M., Venohr, M., Žaloudík, J., 2009. Nitrogen and phosphorus retention in surface waters: An inter-comparison of predictions by catchment models of different complexity. J. Environ. Monit. 11(3), 584. https://doi.org/10.1039/b901207a.

Kovacs, A., Honti, M., Zessner, M., Eder, A., Clement, A., Blöschl, G., 2012. Identification of phosphorus emission hotspots in agricultural catchments. Sci. Total Environ. 433, 74–88. https://doi.org/10.1016/j.scitotenv.2012.06.024.

Liu, G., Chen, L., Wei, G., Shen, Z., 2019. New framework for optimizing best management practices at multiple scales. J. Hydrol. 578, 124133. https://doi.org/10.1016/j.jhydrol.2019.124133.

Miller, B.A., Schaetzl, R.J., 2015. Digital classification of hillslope position. Soil Sci. Soc. Am. J. 79(1), 132–145. https://doi.org/10.2136/sssaj2014.07.0287.

Moriasi, D. N., Arnold, J. G., Van Liew, M. W., Bingner, R. L., Harmel, R. D., Veith, T. L., 2007. Model evaluation guidelines for systematic quantification of accuracy in watershed simulations.

Transactions of the ASABE. 50(3), 885–900. https://doi.org/10.13031/2013.23153.

Nash, J.E., Sutcliffe, J.V., 1970. River flow forecasting through conceptual models part I — A discussion of principles. J. Hydrol. 10(3), 282–290. https://doi.org/10.1016/0022-1694(70)90255-6.

Neitsch, S. L., Arnold, J. G., Kiniry, J. R., Williams, J. R., 2011. Soil and water assessment tool theoretical documentation version 2009. Texas Water Resources Institute.

Pionke, H.B., Gburek, W.J., Sharpley, A.N., 2000. Critical source area controls on water quality in an agricultural watershed located in the Chesapeake Basin. Ecol. Eng. 14(4), 325–335. https://doi.org/10.1016/S0925-8574(99)00059-2.

Qin, C.-Z., Gao, H.-R., Zhu, L.-J., Zhu, A.-X., Liu, J.-Z., Wu, H., 2018. Spatial optimization of watershed best management practices based on slope position units. J. Soil Water Conserv. 73(5), 504–517. https://doi.org/10.2489/jswc.73.5.504.

Qin, C.-Z., Zhu, A.-X., Shi, X., Li, B.-L., Pei, T., Zhou, C.-H., 2009. Quantification of spatial gradation of slope positions. Geomorphology 110, 152–161. https://doi.org/10.1016/j.geomorph.2009.04.003

Rankinen, K., Keinänen, H., Cano Bernal, J.E., 2016. Influence of climate and land use changes on nutrient fluxes from Finnish rivers to the Baltic Sea. Agr. Ecosyst. Environ. 216, 100–115. https://doi.org/10.1016/j.agee.2015.09.010.

Rathjens, H., Bieger, K., Chaubey, I., Arnold, J.G., Allen, P.M., Srinivasan, R., Bosch, D.D., Volk, M., 2016. Delineating floodplain and upland areas for hydrologic models: A comparison of methods. Hydrol. Process. 30(23), 4367–4383. https://doi.org/10.1002/hyp.10918.

Rathjens, H., Oppelt, N., Bosch, D.D., Arnold, J.G., Volk, M., 2015. Development of a grid-based version of the SWAT landscape model. Hydrol. Process. 29(6), 900–914. https://doi.org/10.1002/hyp.10197.

Shang, X., Wang, X., Zhang, D., Chen, W., Chen, X., Kong, H., 2012. An improved SWAT-based computational framework for identifying critical source areas for agricultural pollution at the lake basin scale. Ecol. Model. 226, 1–10. https://doi.org/10.1016/j.ecolmodel.2011.11.030.

Shen, Z., Zhong, Y., Huang, Q., Chen, L., 2015. Identifying non-point source priority management areas in watersheds with multiple functional zones. Water Res. 68, 563–571. https://doi.org/10.1016/j.watres.2014.10.034.

Shi, Y.-X., Zhu, L.-J., Qin, C.-Z., Zhu, A.-X., 2021. Spatial optimization of watershed best management practices based on slope position-field units. Journal of Geo-Information Science 23(4), 564–575. (in Chinese with English abstract). https://doi.org/10.12082/dqxxkx.2021.200335.

Tian, F., Huang, J., Cui, Z., Gao, J., Wang, X, Wang, X, 2020. Integrating multi indices for identifying priority management areas in lowland to control lake eutrophication: A case study in lake Gehu, China. Ecol. Indic. 112, 106103. https://doi.org/10.1016/j.ecolind.2020.106103.

Volk, M., Arnold, J.G., Bosch, D.D., Allen, P.M., Green, C.H., 2007. Watershed configuration and simulation of landscape processes with the SWAT model, in: MODSIM 2007 International Congress on Modelling and Simulation. Modelling and Simulation Society of Australia and New Zealand, Christchurch, New Zealand, pp. 2383–2389.

Wang, G., Chen, L., Huang, Q., Xiao, Y., Shen, Z., 2016. The influence of watershed subdivision level on model assessment and identification of non-point source priority management areas. Ecol. Eng. 87, 110–119. https://doi.org/10.1016/j.ecoleng.2015.11.041.

White, M.J., Storm, D.E., Busteed, P.R., Stoodley, S.H., Phillips, S.J., 2009. Evaluating nonpoint source critical source area contributions at the watershed scale. J. Environ. Qual. 38(4), 1654–1663. https://doi.org/10.2134/jeq2008.0375.

Wolock, D.M., Winter, T.C., McMahon, G., 2004. Delineation and evaluation of hydrologic-landscape regions in the United States using geographic information system tools and multivariate statistical analyses. Environ. Manage. 34, S71–S88. https://doi.org/10.1007/s00267-003-5077-9.

U.S. Environmental Protection Agency. (EPA). 2022. Level III and IV ecoregions of the continental environmental probability. Available online at https://www.epa.gov/eco-research/level-iii-and-iv-ecoregions-state, last updated on May 2, 2022.

Yang, D., Herath, S., Musiake, K., 2002. A hillslope-based hydrological model using catchment area and width functions. Hydrolog. Sci. J. 47(1), 49–65. https://doi.org/10.1080/02626660209492907.

Zhu, L.-J., Qin, C.-Z., Zhu, A.-X., 2021. Spatial optimization of watershed best management practice scenarios based on boundary-adaptive configuration units. Progress in Physical Geography: Earth and Environment 45(2), 207–227. https://doi.org/10.1177/0309133320939002.

Zhu, L.-J., Qin, C.-Z., Zhu, A.-X., Liu, J., Wu, H., 2019. Effects of different spatial configuration units for the spatial optimization of watershed best management practice scenarios. Water 11(2), 262. https://doi.org/10.3390/w11020262.

Table

Table 1. Data description of the study areas for building a SWAT+ model.

	Zhongtianshe Watershed	Willow River Watershed
DEM	DEM with a resolution of 25 m from Provincial Geomatics Centre of Jiangsu	DEM with a resolution of 30 m from National Elevation Data, USGS
Land use	Manually interpreted from a Google Earth image derived in 2015	Land use map from National Land Cover Data (NLCD, 2011 Edition), USGS
Soil	Soil type map obtained from Soil Science Database of China and soil properties from field sampling	Soil dataset from the Soil Survey Geographic database (SSURGO), U.S. Department of Agriculture-Natural Resource Conservation Service
Meteorological data	Daily meteorological data (such as precipitation, temperature, humidity, wind speed, and solar radiation) from 2011 to 2015 provided by China Meteorological Data Service Centre and Liyang Meteorological Station	Daily meteorological data from 2008 to 2014 provided by Climate Forecast System Reanalysis Dataset, U.S. National Centers for Environmental Prediction
Agricultural management practices	Cropping and irrigation schedule including crop types and fertilizer usage from field survey	Crop rotations, tillage practices, and fertilizer usage collated from Almendinger and Murphy (2007)
Observed data at the outlet	Daily measured flow (2011–2015) and 5-day or 3-day* measured total nitrogen data (2014–2015) from the site-monitoring station at the watershed outlet	Daily flow and ammonia plus organic nitrogen data (from 1 October 2010 to 31 July 2014) measured at the monitoring station of the USGS (no. 05341687)

* A total of 181 values were monitored in the Zhongtianshe watershed. During the rainy season (i.e., June to August), the sampling interval is about three days.

Table 2. The SWAT$^+$ model performance for the two study watersheds.

			NSE	PBIAS	RSR	R^2
Zhongtianshe Watershed	Calibration	Flow	0.48	13.36%	0.72	0.52
		Nitrogen	0.27	-16.57%	0.86	0.40
	Validation	Flow	0.52	12.55%	0.69	0.59
		Nitrogen	–	–	–	–
Willow River Watershed	Calibration	Flow	0.48	-28.82%	0.72	0.51
		Nitrogen	0.37	3.97%	0.79	0.39
	Validation	Flow	0.34	-58.16%	0.81	0.47
		Nitrogen	0.25	-128.73%	0.87	0.54

Figure

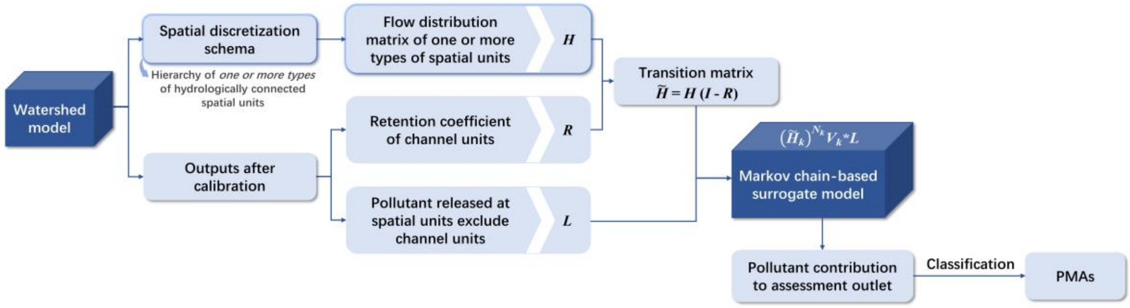

Fig. 1. Generalized framework of the Markov chain-based PMA identification method using a hierarchy of one or more types of hydrologically connected spatial units.

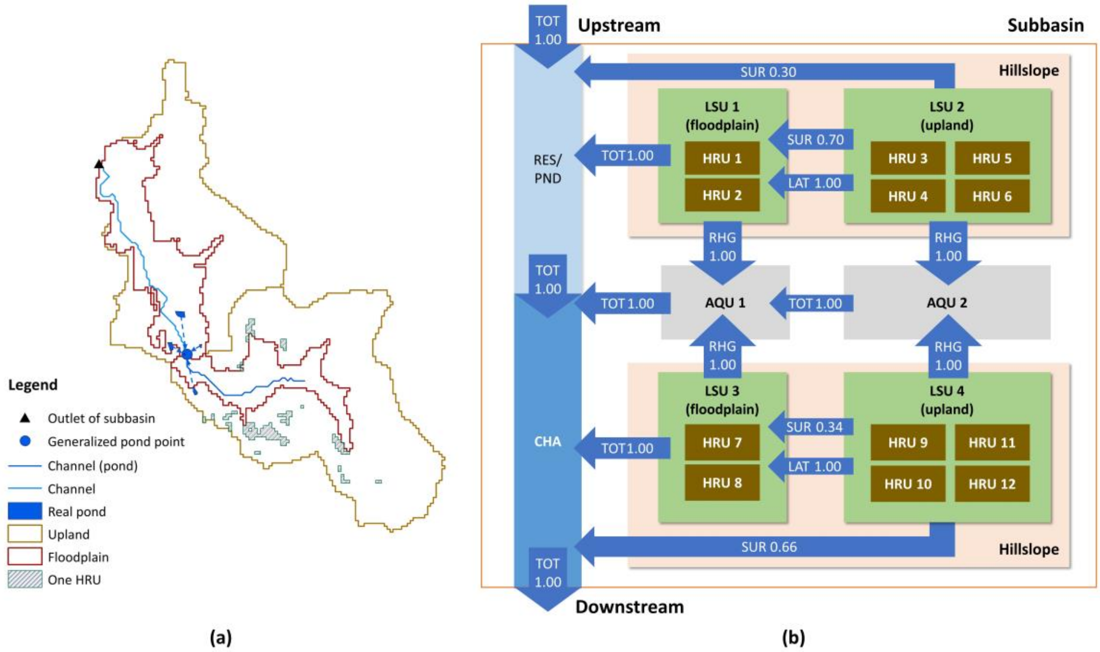

Fig. 2. Schematic of the spatial discretization scheme (a) and hydrologic connections between spatial units (b) implemented in SWAT^{+}. AQU, aquifer; CHA, channel; HRU, hydrologic response unit; LSU, landscape position unit; LAT, lateral flow; PND, pond; RES, reservoir; RHG, groundwater recharge; SUR, surface runoff; TOT, total outflow (specifically, for LSU, it equals to surface runoff plus lateral flow); and numbers represent flow distribution ratio (values less than 1.0 are presented for example) from source unit to receiving unit (adapted from Bieger et al., 2017, 2019, and the source code of SWAT^{+} version 59.3).

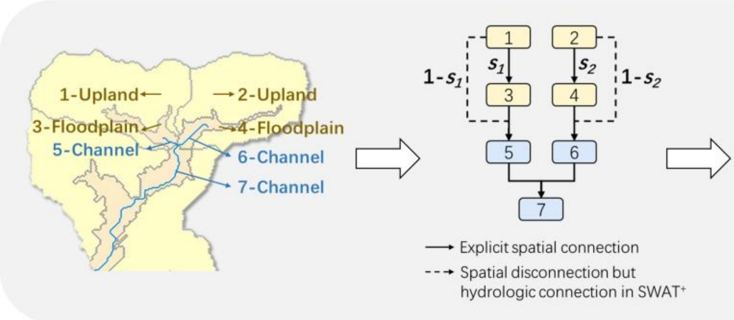

$$H = \begin{vmatrix} 0 & 0 & s_1 & 0 & 1-s_1 & 0 & 0 \\ 0 & 0 & 0 & s_2 & 0 & 1-s_2 & 0 \\ 0 & 0 & 0 & 0 & 1 & 0 & 0 \\ 0 & 0 & 0 & 0 & 0 & 1 & 0 \\ 0 & 0 & 0 & 0 & 0 & 0 & 1 \\ 0 & 0 & 0 & 0 & 0 & 0 & 1 \\ 0 & 0 & 0 & 0 & 0 & 0 & 0 \end{vmatrix}$$

Fig. 3. Example of construction of the flow distribution matrix, *H*, based on upstream-downstream relations among landscape position units (LSUs) and channels and flow distribution ratios from upland to floodplain (e.g., s_1 and s_2 in different subbasins).

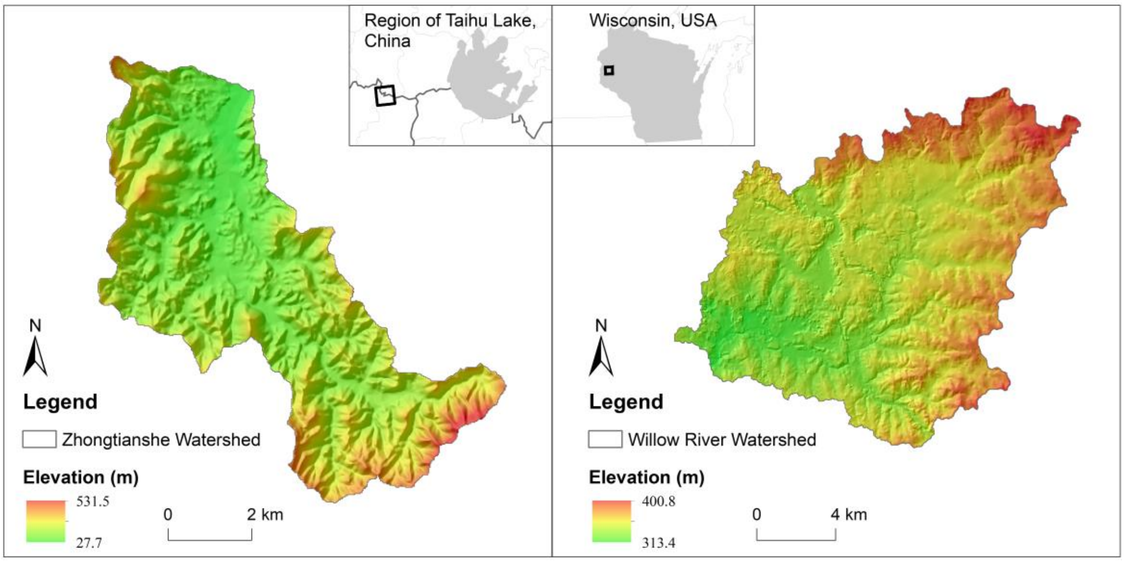

Fig. 4. Overview of the Zhongtianshe and Willow River watersheds.

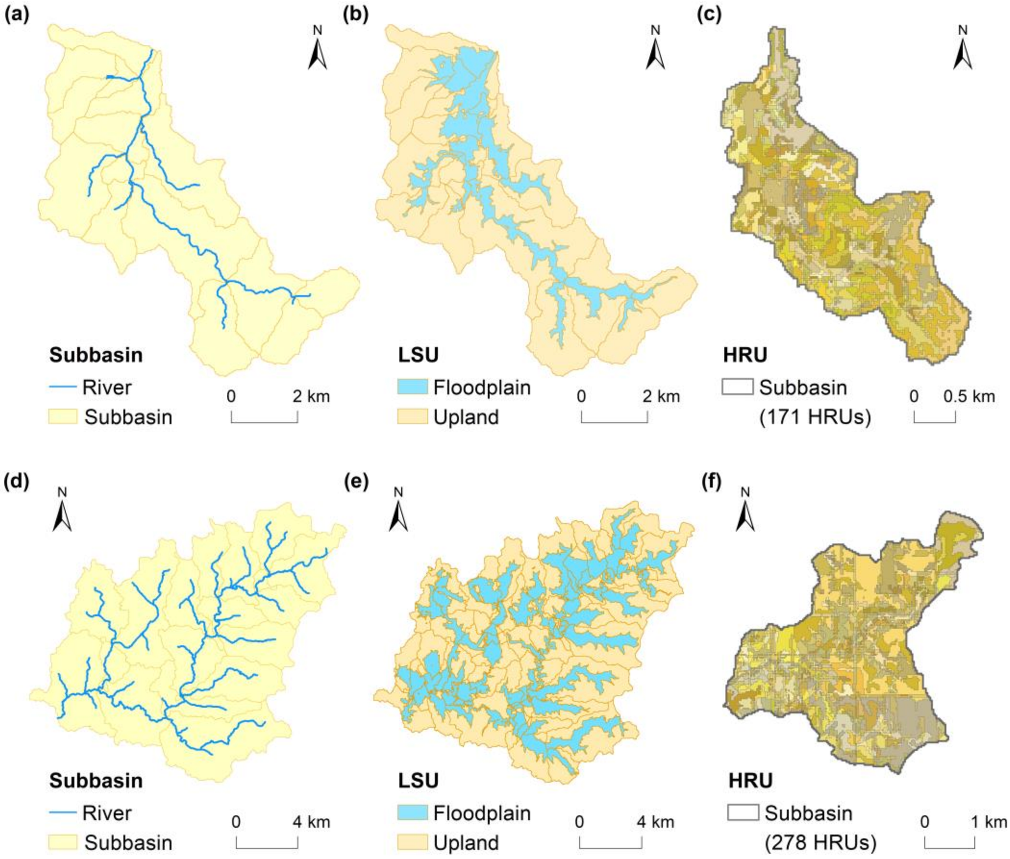

Fig. 5. Delineation of three types of spatial units in the SWAT+ model of the Zhongtianshe Watershed: (a) subbasin, (b) LSU, and (c) HRU (taking one subbasin as an example); and the Willow River Watershed: (d) subbasin, (e) LSU, and (f) HRU (taking one subbasin as an example). Each color within the same subbasin in the HRU map represents one unit, i.e., a particular combination of land use, soil type, and slope classification.

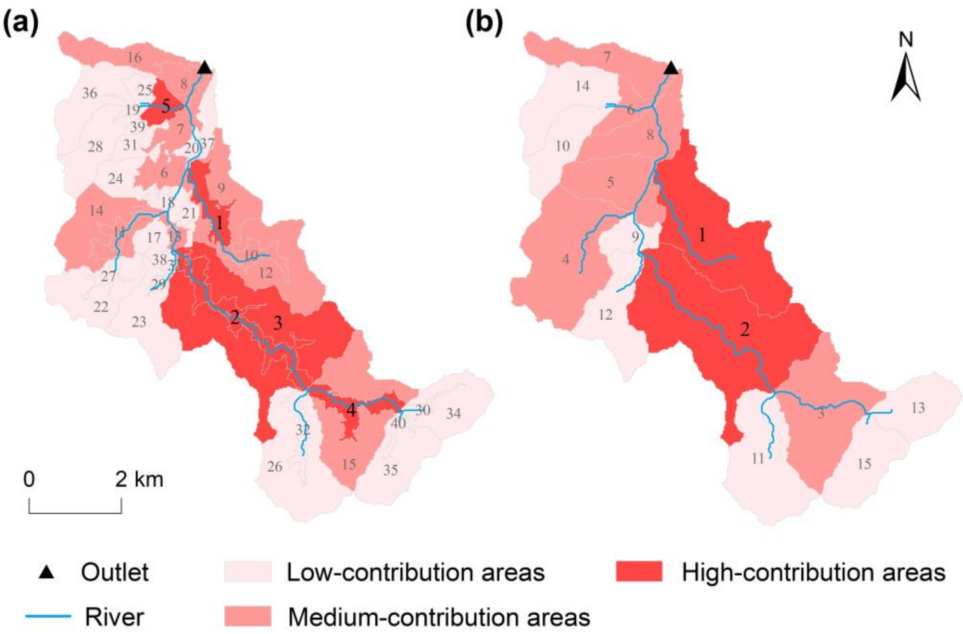

Fig. 6. Ranking and classification of nitrogen load contribution at the (a) LSU (landscape position unit) and (b) subbasin levels in the Zhongtianshe Watershed. The labelled number is the ranked sequence of load contribution in descending order. High-contribution areas are identified as PMAs.

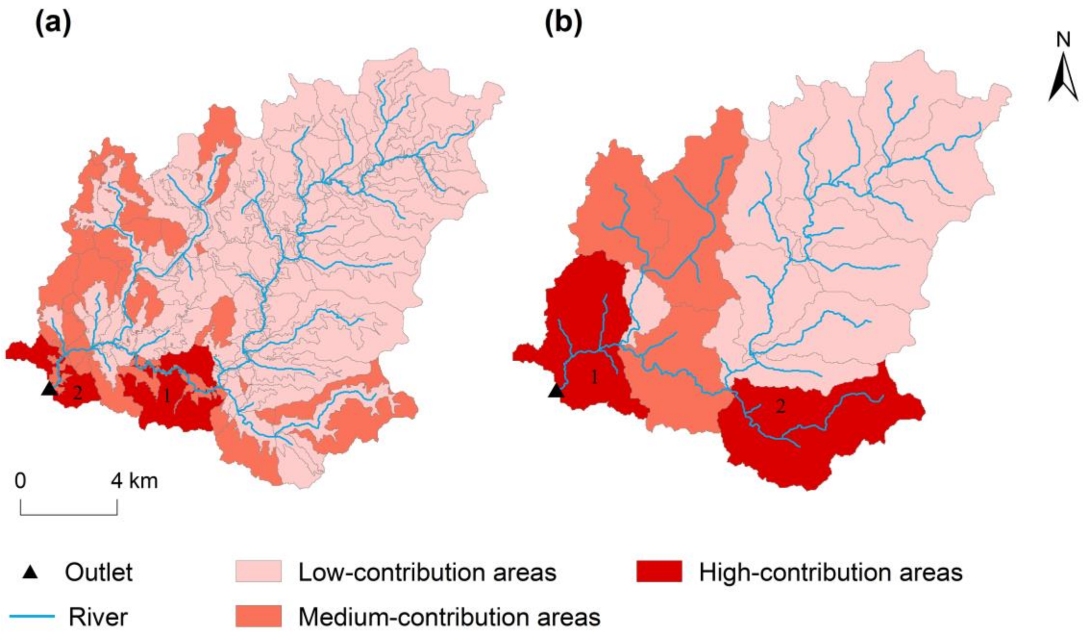

Fig. 7. Ranking and classification of total nitrogen load contribution at the (a) LSU (landscape position unit) and (b) subbasin levels in the Willow River Watershed. High-contribution areas are identified as PMAs, which are ranked and labelled by load contribution.

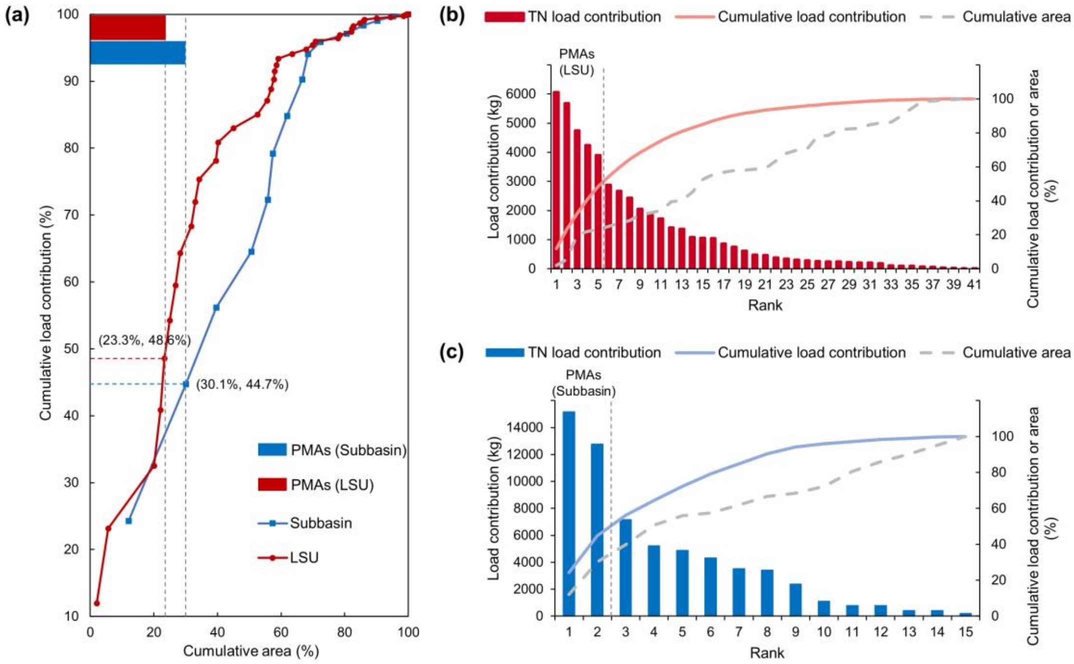

Fig. 8. Relations between cumulative areas of spatial units and corresponding load contributions in the Zhongtianshe Watershed. (a) each point represents a spatial unit arranged in the descending order of load contribution. Detailed load contribution of landscape position units (LSUs) and subbasins are presented in (b) and (c), respectively.

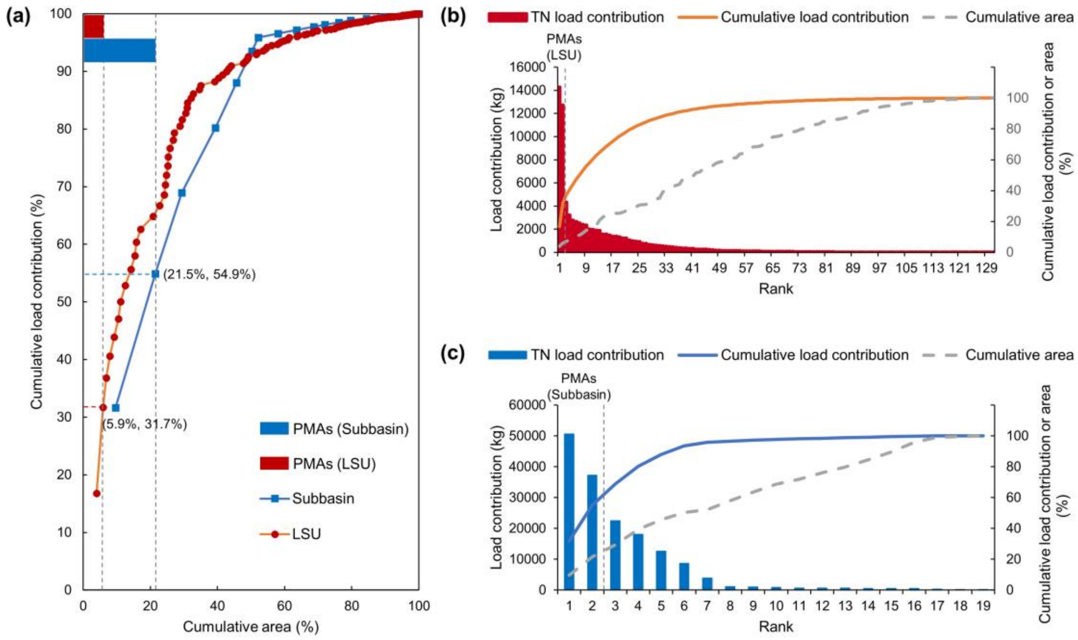

Fig. 9. Relations between cumulative areas of spatial units and corresponding load contributions in the Willow River Watershed. (a) each point represents a spatial unit arranged in the descending order of load contribution. Detailed load contribution of landscape position units (LSUs) and subbasins are presented in (b) and (c), respectively.